

Lucile Dollet,¹ Clara Levrel,¹ Tamer Coskun,² Soazig Le Lay,³ Cedric Le May,¹ Audrey Ayer,¹ Quentin Venara,¹ Andrew C. Adams,² Ruth E. Gimeno,² Jocelyne Magré,¹ Bertrand Cariou,^{1,4,5} and Xavier Prieur^{1,5}



FGF21 Improves the Adipocyte Dysfunction Related to Seipin Deficiency

Diabetes 2016;65:3410–3417 | DOI: 10.2337/db16-0327

Fibroblast growth factor 21 (FGF21) was shown to improve metabolic homeostasis, at least partly by controlling white adipocyte profile and adiponectin secretion. Here, we studied its effect on adipocyte dysfunction in the context of Berardinelli-Seip congenital lipodystrophy (BSCL) linked to seipin deficiency. *Bscl2*^{-/-} mice displayed a progressive adipose tissue loss with aging as evidenced by the altered profile of residual fat pads and the decrease in adiponectin plasma levels in 12- vs. 4-week-old animals. Aiming to prevent this impairment, we treated 6-week-old *Bscl2*^{-/-} mice with an FGF21 analog (LY2405319) for a period of 28 days. FGF21 treatment increased adiponectin plasma levels and normalized insulin sensitivity in *Bscl2*^{-/-} mice by improving the white adipose tissue gene expression pattern. To further decipher the molecular pathways altered by seipin deficiency in mature adipocytes, we developed a unique inducible seipin knockdown cell line (SKD). SKD showed chronic activation of the p38 MAPK pathway associated with apoptotic cell death. Interestingly, FGF21 treatment exerted an antistress effect on SKD cells, reducing p38 MAPK phosphorylation and limiting mature adipocyte loss. Our data demonstrate that FGF21 treatment improves the metabolic profile of *Bscl2*^{-/-} lipodystrophic mice, partly by improving mature adipocyte maintenance through suppression of cellular stress via inhibition of p38 MAPK activity.

Fibroblast growth factor 21 (FGF21) is a hormone highly expressed in liver (1,2). FGF21 was shown to increase

glucose uptake in adipocytes in vitro and subsequently to improve glucose tolerance in obese mice (3). Numerous studies aimed to elucidate the mechanism underlying the metabolic changes observed under FGF21 treatment. FGF21 treatment was shown to induce thermogenesis (4) and glucose uptake in the brown adipose tissue (BAT) and white adipose tissue (WAT) (5). FGF21 stimulates adiponectin production in WAT, and its beneficial effects on insulin sensitivity are lost in adiponectin knockout (KO) mice (6,7). In the context of obesity, these data suggest that FGF21 treatment primarily targets WAT by increasing glucose uptake and stimulating adiponectin secretion, thereby improving the general metabolic status.

Berardinelli-Seip congenital lipodystrophy (BSCL) is characterized by an almost complete lack of adipose tissue associated with severe insulin resistance (8,9). BSCL is a rare genetic disease, with *BSCL2* identified as the first gene involved in 2001 (10). *BSCL2* encodes seipin, an endoplasmic reticulum (ER) transmembrane protein whose cellular function remains poorly understood. Several studies demonstrated that seipin deficiency compromises adipocyte differentiation (11–14). The phenotyping of three independent models of seipin-deficient (*Bscl2*^{-/-}) mice has provided major insights into the pathophysiology of BSCL2 (13–15). These mice display severe lipodystrophy accompanied by a decrease in leptin and adiponectin secretion. The aim of this study was to use FGF21 treatment to correct the adipocyte dysfunction and the metabolic complications associated with seipin deficiency.

¹INSERM UMR S1087/CNRS UMR 6291, l'Institut du Thorax, Université de Nantes, Nantes, France

²Lilly Research Laboratories, Indianapolis, IN

³Stress Oxydant et Pathologies Métaboliques, INSERM UMR 1063, Université d'Angers, Angers, France

⁴Department of Endocrinology, l'Institut du Thorax, CHU de Nantes, Nantes, France

⁵Université de Nantes, Nantes, France

Corresponding author: Xavier Prieur, xavier.prieur@univ-nantes.fr.

Received 10 March 2016 and accepted 14 August 2016.

This article contains Supplementary Data online at <http://diabetes.diabetesjournals.org/lookup/suppl/doi:10.2337/db16-0327/-/DC1>.

B.C. and X.P. equally contributed to this study.

© 2016 by the American Diabetes Association. Readers may use this article as long as the work is properly cited, the use is educational and not for profit, and the work is not altered. More information is available at <http://www.diabetesjournals.org/content/license>.

RESEARCH DESIGN AND METHODS

Animals and LY2405319 Treatment

Bscl2^{-/-} mice were generated as previously described (14). LY2405319 (kindly provided by Lilly) was delivered by osmotic pumps (model 1004; Alzet Inc.). Mice (*n* = 8–11 per group) were killed after a 6-h fasting period. Insulin tolerance tests were performed as previously described (14). Adiponectin plasma levels were measured using ELISA (Crystal Chem, Downers Grove, IL).

Seipin Knockdown Cell Lines

Seipin knockdown was achieved by infecting 3T3-L1 cells with SMARTvector inducible lentiviral short hairpin RNA (Dharmacon, St. Leon-Rot, Germany). A level of 2 μg/mL puromycin selection was maintained throughout the experiments. Adipocyte differentiation protocol was followed (12), but on day 4, doxycycline (5 μg/mL) was added in the indicated wells. Treatment was performed using LY2405319 (500 nmol/L) added at day 6.

Western Blot, Caspase-3 Assay, and RNA Analysis

For Western blot analyses and immunolabeling, we used phosphorylated (p) P38, p-38 MAPK antibodies, and cleaved caspase-3 (Cell Signaling). Caspase-3 activity was evaluated using the N-Acetyl-Asp-Glu-Val-Asp-7-amido-4-methylcoumarin (Ac-DEVD-AMC) caspase-3 substrate that fluoresces following cleavage. RNA expression was analyzed as previously described (14).

Statistical Analysis

All data are reported as mean ± SEM. Data sets were analyzed for statistical significance using the nonparametric Mann-Whitney *U* test, Kruskal-Wallis, or two-way ANOVA analysis.

RESULTS

Seipin Deficiency Affects the Properties of the Mature Adipose Tissue

Bscl2^{-/-} mice were previously shown to display severe lipodystrophy at 3 months of age. Studying these mice at a younger age, we found that WAT loss was progressive. Plasma adiponectin levels decreased by 10-fold between 4 and 14 weeks of age in *Bscl2*^{-/-} mice, concomitantly with the worsening of random-fed hyperglycemia (Fig. 1A and B). A 50% decrease in inguinal fat pad weight and a complete disappearance of the gonadal fat pad were observed in *Bscl2*^{-/-} mice between 4 and 12 weeks of age (Fig. 1C). Gene expression of several mature adipocyte markers (*PPARγ*, *Adipoq*, *aP2*, *Hsl*, and *Plin1*) were significantly decreased in inguinal WAT from 12-week-old compared with 4-week-old *Bscl2*^{-/-} mice (Fig. 1D). Transmission electron microscopy imaging of WAT from 4-week-old *Bscl2*^{-/-} mice revealed the presence of autophagic vacuoles and extended ER tubular network (Fig. 1E). Finally, ex vivo caspase-3 activity (Fig. 1F) and immunohistochemistry with cleaved caspase-3 staining (Fig. 1G) indicated a high level of apoptosis in adipocytes. These observations suggest that seipin-deficient WAT is undergoing cellular stress, compromising its functionality.

FGF21 Is Overexpressed in WAT of Young *Bscl2*^{-/-} Mice

Fgf21 mRNA levels were strongly increased in 4-week-old *Bscl2*^{-/-} mice compared with wild-type mice but were decreased over time in 12-week-old *Bscl2*^{-/-} mice (Fig. 1H). Pioglitazone treatment, which improves both WAT gene expression pattern and metabolic profile in *Bscl2*^{-/-} mice (14), increased *Fgf21* mRNA levels in *Bscl2*^{-/-} WAT (Fig. 1I). On the basis of these results, we hypothesized that FGF21 might counteract the adipocyte dysfunction related to seipin deficiency.

FGF21 Treatment Improves the Metabolic Complications in *Bscl2*^{-/-} Mice

We treated 6-week-old *Bscl2*^{-/-} and *Bscl2*^{+/+} mice with the FGF21 analog LY2405319 for a period of 4 weeks. LY2405319 reduced the random-fed glucose levels in *Bscl2*^{+/+} mice and corrected the hyperglycemia in *Bscl2*^{-/-} mice (Fig. 2A). LY2405319 improved insulin sensitivity (Fig. 2B) and induced a 2.5-fold increase in plasma adiponectin levels (Fig. 2C) in *Bscl2*^{-/-} mice (1,562 ± 164 mg/mL vs. 636 ± 48 mg/mL). LY2405319 increased the mRNA expression of mature adipocyte markers in the inguinal WAT from *Bscl2*^{-/-} mice, including *aP2*, *Pparγ*, *Hsl*, *Atgl*, *Lep*, and *Adipoq* (Fig. 2F), without a significant change in adipose tissue mass (Fig. 2D and E). In addition, LY2405319 increased *Ucp1* and *Pgc1a* mRNA levels (two- and threefold, respectively) in *Bscl2*^{-/-} WAT but not in BAT (Supplementary Fig. 1A). LY2405319 did not alter hepatic triglyceride content or the catabolic gene expression pattern and had only a mild lowering effect on the mRNA levels of the lipogenic genes *Scd1* and *Chrebp* in the liver (Supplementary Fig. 1C–E).

We next treated older *Bscl2*^{-/-} mice that already displayed metabolic abnormalities. FGF21-treated mice maintained their initial adiponectin levels, whereas nontreated animals displayed a 2.5-fold decrease of plasma adiponectin levels (Fig. 2G). In older *Bscl2*^{-/-} mice, the effect of FGF21 on random-fed glycemia was milder and the improvement of insulin sensitivity failed to achieve statistical significance (Supplementary Fig. 2A and B).

Altogether these results demonstrate that FGF21 treatment is able to prevent the WAT dysfunction associated with seipin deficiency, i.e., to increase adiponectin secretion and to improve the metabolic profile of young *Bscl2*^{-/-} mice.

FGF21 Improves Maintenance of Seipin-Deficient Mature Adipocytes

To assess whether FGF21 might directly correct the adipocyte dysfunction due to seipin deficiency, we generated a cell line derived from 3T3-L1 preadipocytes with conditional *Bscl2* knockdown (SKD). Because seipin is required for full adipocyte differentiation (11–14), this cell model allowed us to study the effect of seipin deficiency in mature adipocytes. Using Oil Red O staining, we observed that at day 8 the differentiation levels (~90%) were identical in all conditions (Supplementary Fig. 3A and B). *Adipoq* and *aP2* expression levels were similar in all conditions, whereas doxycycline-treated SKD displayed

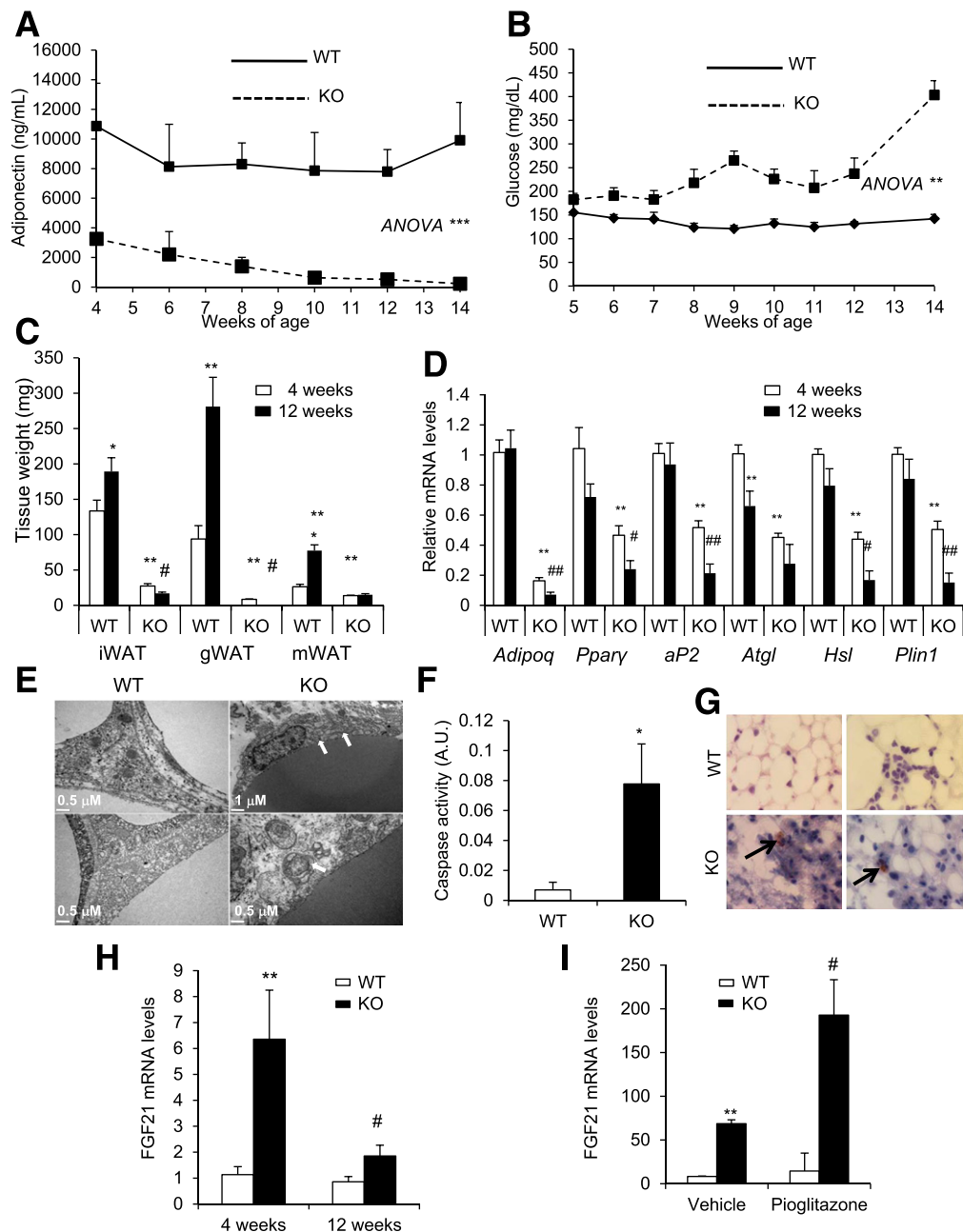


Figure 1—Seipin deficiency affects the properties of the mature adipose tissue. **A** and **B**: Progression of plasma adiponectin levels (**A**) and random-fed glycemia (**B**) in *Bscl2*^{+/+} mice (wild type [WT], solid lines) and *Bscl2*^{-/-} mice (KO, dashed lines) from 4 to 14 weeks of age. **C**: Mass of inguinal WAT (iWAT), gonadal WAT (gWAT), and mesenteric WAT (mWAT) from *Bscl2*^{+/+} and *Bscl2*^{-/-} mice at 4 (white bars) or 12 weeks of age (black bars). **D**: Gene expression profile of inguinal WAT of *Bscl2*^{+/+} and *Bscl2*^{-/-} mice at 4 (white bars) and 12 weeks of age (black bars) ($n = 6$ per group). **E**: Transmission electronic microscopic images of 4-week-old *Bscl2*^{+/+} and *Bscl2*^{-/-} inguinal WAT. The arrows indicate autophagic vacuoles and extended ER. **F**: Caspase-3 activity measured in inguinal WAT from 4-week-old *Bscl2*^{+/+} (white bars) and *Bscl2*^{-/-} (black bars) mice. **G**: Immunohistochemistry with cleaved caspase-3 antibody in paraffin-embedded inguinal WAT from 4-week-old *Bscl2*^{+/+} and *Bscl2*^{-/-} mice. Arrows indicate the cleaved caspase-3-positive cells. **H**: *Fgf21* mRNA levels in inguinal WAT from 4- or 12-week-old *Bscl2*^{+/+} (white bars) and *Bscl2*^{-/-} (black bars) mice. **I**: *Fgf21* mRNA levels in inguinal WAT from *Bscl2*^{+/+} (white bars) and *Bscl2*^{-/-} (black bars) mice treated or not with pioglitazone for 8 weeks. A.U., arbitrary unit. Error bars represent SEM. Significant differences between *Bscl2*^{+/+} and *Bscl2*^{-/-} mice are represented as follows: * $P < 0.05$, ** $P < 0.01$, and *** $P < 0.001$. Significant differences between 4- and 12-week-old mice are represented as follows: # $P < 0.05$ and ## $P < 0.01$.

an 80% reduction in *Bscl2* mRNA levels, validating our mature adipocyte seipin-deficient model (Fig. 3A). At day 21, SKD doxycycline-treated cells displayed a strong reduction in *Adipoq* and *aP2* mRNA levels (Fig. 3B) and a decrease in Oil Red O-positive cells (Fig. 3C), suggesting a progressive

loss of mature adipocytes. We then investigated some other stress-activated signaling pathways that may potentially be involved in this apoptotic response. We noticed that seipin deficiency did not alter the phosphorylation levels of JNK and EIF2A (ER stress key player) (data not shown).

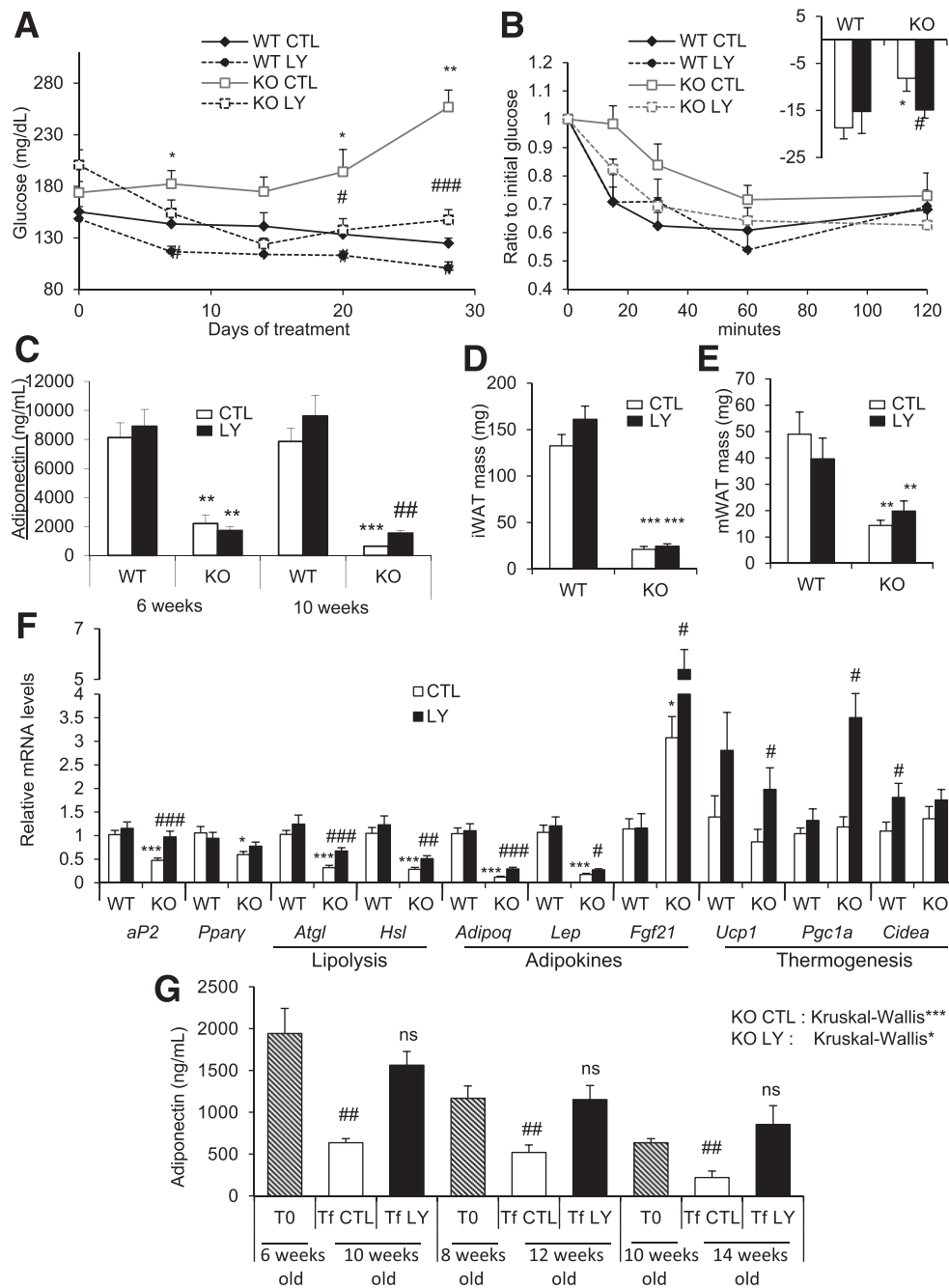


Figure 2—FGF21 treatment improves the metabolic complications in *Bsc2*^{-/-} mice. Osmotic pumps were implanted on day 0 delivering 1 mg/kg/day for 28 days of LY2405319 (LY). **A**: Random-fed glycemia during 28 days in 6-week-old *Bsc2*^{+/+} (wild type [WT]) (solid line, black diamond, control [CTL], *n* = 9; dashed line, black diamond, LY, *n* = 9) and *Bsc2*^{-/-} (KO) mice (solid line, white square, CTL, *n* = 11; dashed line, white square, LY, *n* = 10). **B**: Insulin tolerance test performed at day 24 of experiment. The bar graph shows the area under curve. **C**: Plasma adiponectin levels in *Bsc2*^{-/-} mice treated with (black bars) or without (white bars) the FGF21 analog for a period of 4 weeks. Inguinal WAT (iWAT) (**D**) and mesenteric WAT (mWAT) (**E**) mass from *Bsc2*^{+/+} and *Bsc2*^{-/-} mice treated with LY2405319 (black bars) or not (white bars). **F**: Gene expression profile of inguinal WAT from *Bsc2*^{+/+} and *Bsc2*^{-/-} mice treated with (black bars) or without (white bars) the FGF21 analog LY2405319. **G**: Experiments were performed with 6-, 8-, and 10-week-old mice, and adiponectin was measured at T0 and after a 4-week treatment with FGF21 (Tf). Error bars represent SEM. Significant differences between *Bsc2*^{+/+} and *Bsc2*^{-/-} mice were represented as follows: **P* < 0.05, ***P* < 0.01, and ****P* < 0.001. Significant differences between control and LY2405319 conditions were represented as follows: #*P* < 0.05, ##*P* < 0.01, and ###*P* < 0.001.

However, doxycycline-treated SKD cells displayed a threefold increase in p38 MAPK phosphorylation as well as a 2.5 induction in the mRNA levels of one of its target genes, the death receptor FASR (16) (Fig. 3D–F). Seipin-deficient

mature adipocytes displayed a sevenfold increase in caspase-3 activity (Fig. 3G) and stained positively for both cleaved caspase-3 and bodipy (lipid droplets) (Supplementary Fig. 3C). It is noteworthy that treatment with the p38 MAPK inhibitor

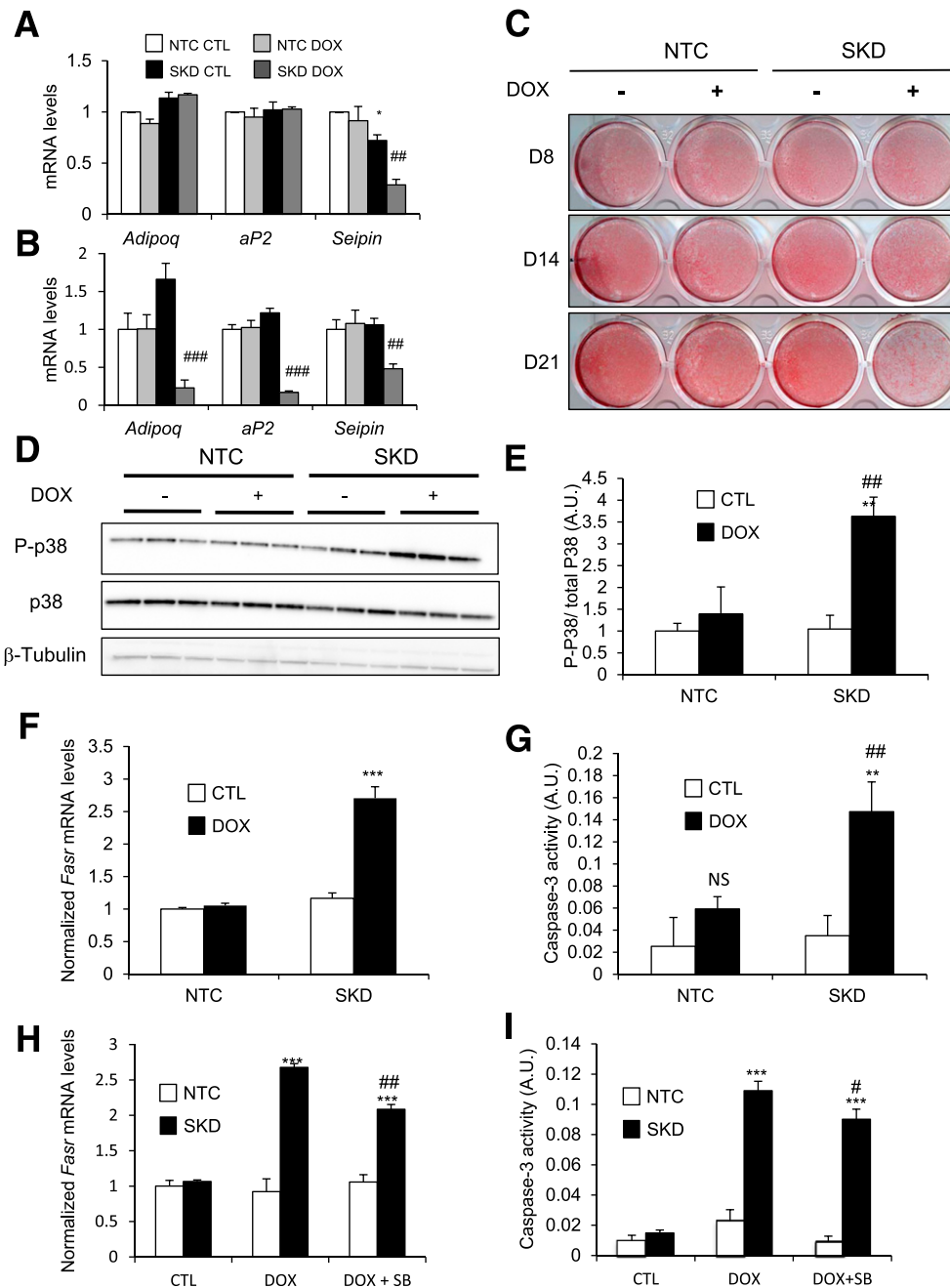


Figure 3—Seipin deficiency in mature adipocytes. Nontargeted control (NTC) and seipin knockdown (SKD) cells were differentiated for 8 days and maintained in culture until day 21. Doxycycline was added at day 4 and maintained until day 21. *A* and *B*: Gene expression profile of NTC and SKD adipocytes with or without doxycycline treatment at day 8 (*A*) and day 21 (*B*). *C*: Oil Red O staining of NTC and SKD adipocytes at 8, 14, and 21 days after the initiation of differentiation in absence (CTL) or in presence (DOX) of 5 $\mu\text{g}/\mu\text{L}$ doxycycline treatment. Western blot representing phosphorylated levels of p38 MAPK (*D*) and quantification (*E*). *Fasn* mRNA levels (*F*) and caspase-3 activity (*G*) at day 14 with (black bars) or without (white bars) doxycycline treatment in NTC and SKD cells. p38 MAPK inhibitor SB203580 (SB) (2.5 $\mu\text{mol}/\text{L}$) was added at day 8 and the *Fasn* mRNA levels (*H*) and caspase-3 activity (*I*) at day 14 are shown. A.U., arbitrary unit. Error bars represent SEM. Significant differences between NTC and SKD cells were represented as follows: * $P < 0.05$, ** $P < 0.01$, and *** $P < 0.001$. Significant differences between control and doxycycline conditions were represented as follows: # $P < 0.05$, ## $P < 0.01$, and ### $P < 0.001$.

SB203580 decreased by 35% the induction of *Fasn* mRNA expression and decreased by 20% the caspase-3 activity in seipin-deficient cells (Fig. 3*H* and *I*).

We tested whether FGF21 could directly prevent the loss of mature seipin-deficient adipocytes. Oil Red O staining at day 21 of differentiation revealed that LY2405319 treatment

(from day 6) partially prevented adipocyte loss (Fig. 4*A* and *B*). LY2405319 maintained *Adipoq* and *aP2* mRNA expression levels (Fig. 4*C* and *D*, respectively). In addition, LY2405319 was able to reduce p38 activation, caspase-3 activity, and *Fasn* mRNA levels in doxycycline-treated SKD adipocytes (Fig. 4*E*–*G*). Finally, we demonstrated that LY2405319 was able

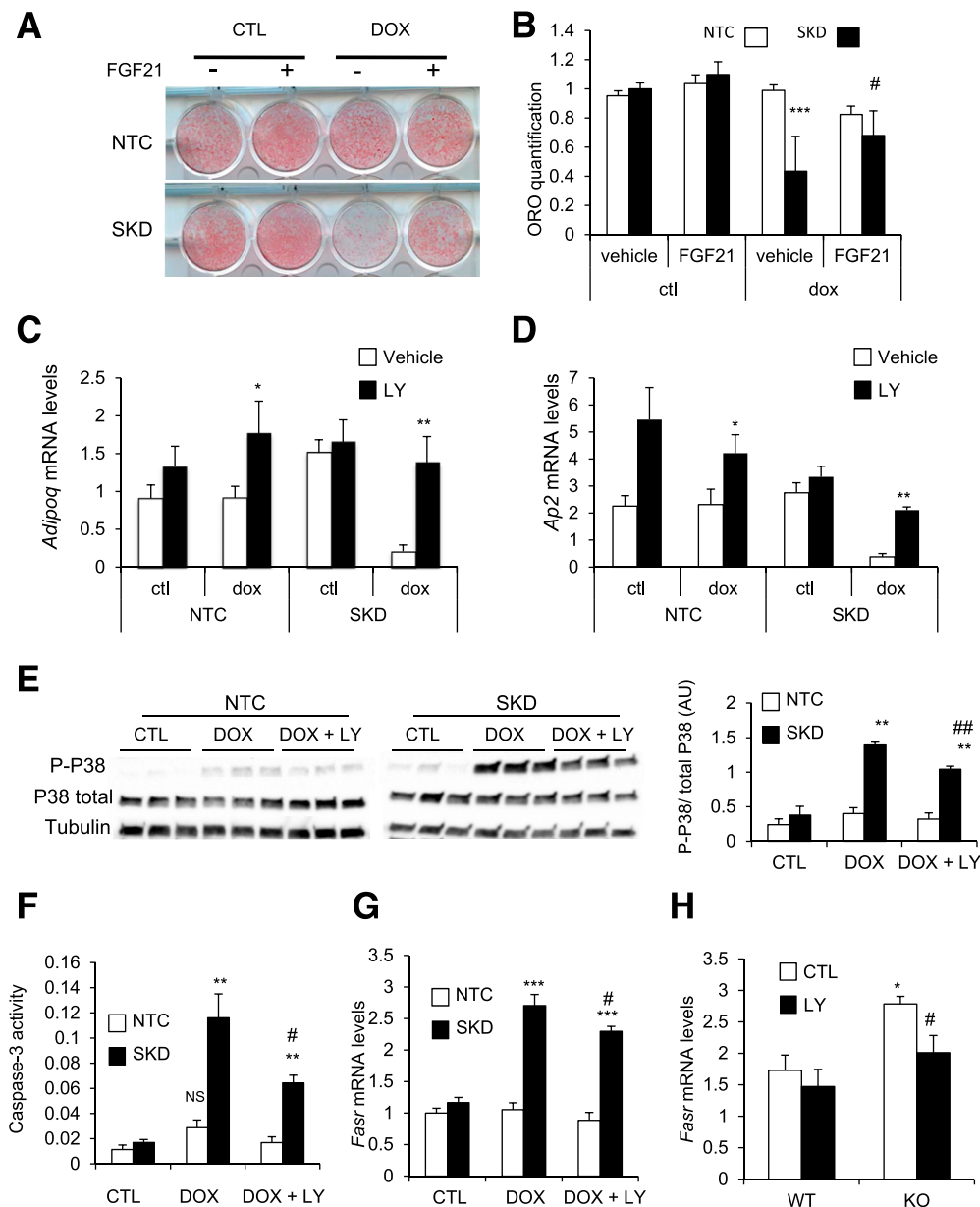


Figure 4—FGF21 treatment prevents seipin-deficient adipocyte loss. FGF21 analog LY2405319 (LY) (500 nmol/L) was added at day 6 after the initiation of differentiation. Images of Oil Red O (ORO) staining at day 21 of nontargeted control (NTC) and seipin knockdown (SKD) cells with or without FGF21 treatment (A) and quantification (B). C and D: Gene expression profile at day 21 in NTC and SKD cells treated (black bars, LY) or not (white bars, control [CTL]) with the FGF21 analog. E: Western blot representing phosphorylated levels of p38 MAPK and quantification. Measurement of caspase-3 activity (F) and *Fasn* mRNA levels (G) at day 14 with or without doxycycline (DOX) treatment in NTC (white bars) and SKD (black bars) cells. H: *Fasn* mRNA levels in inguinal WAT from *Bscl2*^{+/+} and *Bscl2*^{-/-} mice treated (black bars, LY) or not (white bars, CTL) with the FGF21 analog LY2405319. AU, arbitrary unit. Error bars represent SEM. Significant differences between NTC and SKD cells were represented as follows: **P* < 0.05, ***P* < 0.01, and ****P* < 0.001. Significant differences between control and doxycycline conditions were represented as follows: #*P* < 0.05 and ##*P* < 0.01.

to reduce *Fasn* mRNA levels in vivo in WAT from *Bscl2*^{-/-} mice (Fig. 4H).

DISCUSSION

We assessed whether treatment with FGF21 analog was able to correct the metabolic abnormalities associated with seipin deficiency (i.e., BSCL2), the most severe form of lipodystrophy. We showed that FGF21 prevents the progressive

dysfunction of WAT in *Bscl2*^{-/-} mice, potentiating an improvement in insulin sensitivity. Those effects appear to be mainly mediated by the WAT. By using a unique cellular model of seipin knockdown in differentiated adipocytes, we demonstrated that seipin is critical for the maintenance of mature adipocytes. Indeed, seipin deficiency is associated with cellular stress activation and apoptosis that can be partly prevented by FGF21 treatment.

Whether lipodystrophy is due exclusively to an alteration in the development of adipose tissue or to its rapid disappearance remains unknown. MRI exploration in BSCL patients sometimes shows residual WAT (17). To date, seipin deficiency has been mainly shown to impair adipogenesis and to increase unstimulated basal lipolysis (13,14,18,19). In this report, we show for the first time that there is a loss of adipose tissue in *Bscl2*^{-/-} mice between 4 and 12 weeks of age, meaning that the adipogenesis impairment cannot alone explain the lipodystrophic phenotype previously described in adult mice. In vitro, inducible seipin knockdown in fully mature adipocytes increases p38 MAPK phosphorylation and caspase-3 activity, both indicative of a substantial loss of mature adipocytes. The double staining of cleaved caspase-3 and bodipy demonstrates that apoptosis is taking place in the mature adipocyte. Chronic treatment with a low dose of the p38 inhibitor SB203580 significantly reduces the *Fasr* mRNA induction and the caspase-3 activity, supporting the notion that p38 MAPK activation contributes at least partly to the induction of apoptosis observed in doxycycline-treated SKD cells. However, the effects of SB203580 failed to fully restore the phenotype of SKD cells. This could be explained by the lower dose used here to avoid cellular toxicity upon a chronic treatment (i.e., 2.5 $\mu\text{mol/L}$ compared with 20 $\mu\text{mol/L}$ in acute studies [20]). Alternatively, this could indicate that some p38 MAPK-independent pathways contribute to the apoptosis in these cells. Our results are consistent with two recent studies reporting that in vivo seipin deficiency in mature adipocytes leads to progressive lipodystrophy (21,22). Although further studies are needed to highlight the causes of the cellular stress, it is tempting to speculate that apoptosis induction takes part in the adipocyte loss in vivo and contributes to the lipodystrophic phenotype.

The observation that FGF21 expression is transiently induced in WAT of 4-week-old *Bscl2*^{-/-} mice led us to hypothesize that FGF21 might be locally overexpressed as a compensatory response to tissue stress. Importantly, pharmacological treatment with the FGF21 analog LY2405319 is able to prevent the progressive decrease in adiponectin secretion and the deterioration of the WAT expression pattern. This might explain the unexpected increase in *Fgf21* expression levels in *Bscl2*^{-/-} mice only. Indeed, in *Bscl2*^{-/-} mice from 4 to 12 weeks of age, there was a threefold decrease in *Fgf21* mRNA levels along with the degradation of the WAT. LY2405319 prevented this degradation and might therefore maintain the *Fgf21* mRNA levels at their steady state, resulting in a 2.5-fold increase in 12-week-old *Bscl2*^{-/-} mice treated with LY2405319 compared with untreated ones. When we treated 6-week-old *Bscl2*^{-/-} mice that display only a threefold decrease in adiponectin levels with LY2405319, we were able to improve insulin sensitivity and hyperglycemia. Previous reports have shown that the metabolic effects of FGF21 are mediated by an increase in adiponectin production, as the metabolic efficacy of FGF21 is abolished in adiponectin-deficient mice (6,7). Notably, when

we treated older mice (i.e., 8 weeks old) that display a 10-fold decrease in adiponectin circulating levels, FGF21 treatment still prevented a further decrease in plasma adiponectin concentrations but failed to improve insulin sensitivity. Previous results showed that FGF21 treatment does not improve glucose tolerance in lipodystrophic aP2-nuclear SREBP1c mice. In the same study, WAT transplantation restored the beneficial effects of FGF21 (23). In our study, WAT appears to be the main target of FGF21 as there is no major effect on the BAT or the liver. Regarding the lack of effect on BAT, this is consistent with two recent reports showing that FGF21 similarly improves glucose homeostasis in wild-type and UCP1 KO mice (24,25). Altogether, these data support the hypothesis that WAT is the key mediator of the beneficial effect of FGF21 and that a minimum amount of functional WAT is required to enable its effect.

Finally, we demonstrate that in vitro FGF21 treatment is able to maintain adiponectin mRNA levels, to reduce p38 MAPK chronic activation, and to limit the mature adipocyte loss. As the strongest effect of FGF21 treatment is on the induction of *Adipoq* mRNA, we may assume that adiponectin exerts an anticellular stress autocrine effect, as previously suggested (26,27). Further works are required to demonstrate the direct effect of adiponectin on p38 activation and apoptosis induction. Nevertheless, these in vitro results are consistent with those in vivo that place adiponectin at the center of the beneficial effect of FGF21 in our lipodystrophic model. As LY2405319 treatment lowers FAS-R expression in *Bscl2*^{-/-} WAT, it is tempting to speculate that FGF21 limits the apoptosis induction in vivo.

To our knowledge, this is the first report suggesting that a FGF21 analog might exert its protective effect in WAT through an anticellular stress effect on mature adipocytes. Our study is important not only for the metabolic complications associated with BSCL2 but also for the adipocyte dysfunction in the context of obesity and metabolic syndrome. Notably, from a clinical perspective regarding lipodystrophic patients, we might speculate that the FGF21 analog represents a novel therapeutic approach if used at an early stage of the disease or in patients with partial lipodystrophy.

Acknowledgments. The authors thank M. Takahashi, J.-F. Deleuze, and M. Lathrop (Centre d'Energie Atomique, Centre de Génotypage, Evry, France) for donating the mouse model and C. Dumet, S. Suzanne, and S. Lemarchand-Minde (Animal Facility, l'Institut du Thorax, Nantes, France) for animal care. The authors thank Lisa Oliver for her precious advice for the caspase-3 assay. They also thank the MicroPICell core facility (Structure Fédérative de Recherche François Bonamy, Nantes, France) for microscopy and Guillaume Mabileau for helpful technical assistance for transmission electron microscopy performed at SCIAM (Service Commun Imagerie et d'Analyse Microscopique), Université d'Angers.

Funding. This work was supported by grants from the INSERM and the French associations Association pour la Recherche sur le Diabète, Société Francophone du Diabète, and Fondation de France. L.D. is supported by a PhD fellowship from Ministère de la Recherche et de la Technologie. C.L. is funded by

a PhD fellowship from the region Pays de la Loire and INSERM Grand Ouest. X.P. was awarded the European Foundation for the Study of Diabetes/Lilly Research Fellowship Programme 2015. LY2405319 was provided by Lilly.

Duality of Interest. T.C., A.C.A., and R.E.G. are Lilly employees involved in LY2405319 development. B.C. has received research funding from Sanofi; has received honoraria from Amgen, AstraZeneca, Pierre Fabre, Janssen, Eli Lilly, Merck Sharp & Dohme, Novo Nordisk, Sanofi, and Takeda; and has acted as a consultant/advisory panel member for Amgen, Eli Lilly, Merck Sharp & Dohme, Novo Nordisk, Sanofi, and Regeneron. No other potential conflicts of interest relevant to this article were reported.

Author Contributions. L.D. researched data and wrote the manuscript. C.L., S.L.L., A.A., and Q.V. researched data. T.C., A.C.A., and R.E.G. contributed to the scientific discussion and edited the manuscript. C.L.M. contributed to scientific discussion. J.M. wrote the manuscript. B.C. contributed to scientific design and wrote the manuscript. X.P. researched data, designed the experiments, and wrote the manuscript. X.P. is the guarantor of this work and, as such, had full access to all the data in the study and takes responsibility for the integrity of the data and the accuracy of the data analysis.

References

- Badman MK, Pissios P, Kennedy AR, Koukos G, Flier JS, Maratos-Flier E. Hepatic fibroblast growth factor 21 is regulated by PPARalpha and is a key mediator of hepatic lipid metabolism in ketotic states. *Cell Metab* 2007;5:426–437
- Inagaki T, Dutchak P, Zhao G, et al. Endocrine regulation of the fasting response by PPARalpha-mediated induction of fibroblast growth factor 21. *Cell Metab* 2007;5:415–425
- Kharitonov A, Shiyonova TL, Koester A, et al. FGF-21 as a novel metabolic regulator. *J Clin Invest* 2005;115:1627–1635
- Coskun T, Bina HA, Schneider MA, et al. Fibroblast growth factor 21 corrects obesity in mice. *Endocrinology* 2008;149:6018–6027
- Emanuelli B, Vienberg SG, Smyth G, et al. Interplay between FGF21 and insulin action in the liver regulates metabolism. *J Clin Invest* 2014;124:515–527
- Holland WL, Adams AC, Brozinick JT, et al. An FGF21-adiponectin-ceramide axis controls energy expenditure and insulin action in mice. *Cell Metab* 2013;17:790–797
- Lin Z, Tian H, Lam KS, et al. Adiponectin mediates the metabolic effects of FGF21 on glucose homeostasis and insulin sensitivity in mice. *Cell Metab* 2013;17:779–789
- Garg A. Clinical review: lipodystrophies: genetic and acquired body fat disorders. *J Clin Endocrinol Metab* 2011;96:3313–3325
- Capeau J, Magré J, Caron-Debarle M, et al. Human lipodystrophies: genetic and acquired diseases of adipose tissue. *Endocr Dev* 2010;19:1–20
- Magré J, Delépine M, Khallouf E, et al.; BSCL Working Group. Identification of the gene altered in Berardinelli-Seip congenital lipodystrophy on chromosome 11q13. *Nat Genet* 2001;28:365–370
- Chen W, Yechoor VK, Chang BH, Li MV, March KL, Chan L. The human lipodystrophy gene product Berardinelli-Seip congenital lipodystrophy 2/seipin plays a key role in adipocyte differentiation. *Endocrinology* 2009;150:4552–4561
- Payne VA, Grimsey N, Tuthill A, et al. The human lipodystrophy gene BSCL2/seipin may be essential for normal adipocyte differentiation. *Diabetes* 2008;57:2055–2060
- Chen W, Chang B, Saha P, et al. Berardinelli-Seip congenital lipodystrophy 2/seipin is a cell-autonomous regulator of lipolysis essential for adipocyte differentiation. *Mol Cell Biol* 2012;32:1099–1111
- Prieur X, Dollet L, Takahashi M, et al. Thiazolidinediones partially reverse the metabolic disturbances observed in Bsc12/seipin-deficient mice. *Diabetologia* 2013;56:1813–1825
- Cui X, Wang Y, Tang Y, et al. Seipin ablation in mice results in severe generalized lipodystrophy. *Hum Mol Genet* 2011;20:3022–3030
- Porrás A, Zuluaga S, Black E, et al. P38 alpha mitogen-activated protein kinase sensitizes cells to apoptosis induced by different stimuli. *Mol Biol Cell* 2004;15:922–933
- Hegele RA, Joy TR, Al-Attar SA, Rutt BK. Thematic review series: adipocyte biology. Lipodystrophies: windows on adipose biology and metabolism. *J Lipid Res* 2007;48:1433–1444
- Sim MF, Talukder MU, Dennis RJ, Edwardson JM, Rochford JJ. Analyzing the functions and structure of the human lipodystrophy protein seipin. *Methods Enzymol* 2014;537:161–175
- Dollet L, Magré J, Cariou B, Prieur X. Function of seipin: new insights from Bsc12/seipin knockout mouse models. *Biochimie* 2014;96:166–172
- Wang XZ, Ron D. Stress-induced phosphorylation and activation of the transcription factor CHOP (GADD153) by p38 MAP Kinase. *Science* 1996;272:1347–1349
- Liu L, Jiang Q, Wang X, et al. Adipose-specific knockout of SEIPIN/BSCL2 results in progressive lipodystrophy. *Diabetes* 2014;63:2320–2331
- Zhou H, Lei X, Benson T, et al. Berardinelli-Seip congenital lipodystrophy 2 regulates adipocyte lipolysis, browning, and energy balance in adult animals. *J Lipid Res* 2015;56:1912–1925
- Véniant MM, Hale C, Helmering J, et al. FGF21 promotes metabolic homeostasis via white adipose and leptin in mice. *PLoS One* 2012;7:e40164
- Véniant MM, Sivits G, Helmering J, et al. Pharmacologic effects of FGF21 are independent of the “browning” of white adipose tissue. *Cell Metab* 2015;21:731–738
- Samms RJ, Smith DP, Cheng CC, et al. Discrete aspects of FGF21 in vivo pharmacology do not require UCP1. *Cell Reports* 2015;11:991–999
- Turer AT, Scherer PE. Adiponectin: mechanistic insights and clinical implications. *Diabetologia* 2012;55:2319–2326
- Ajuwon KM, Spurlock ME. Adiponectin inhibits LPS-induced NF-kappaB activation and IL-6 production and increases PPARgamma2 expression in adipocytes. *Am J Physiol Regul Integr Comp Physiol* 2005;288:R1220–R1225